

# Thymol Isolated from *Thymus vulgaris* L. Inhibits Colorectal Cancer Cell Growth and Metastasis by Suppressing the Wnt/ $\beta$ -Catenin Pathway

This article was published in the following Dove Press journal:  
*Drug Design, Development and Therapy*

Qiongyao Zeng<sup>1,2</sup>  
Yuncheng Che<sup>2</sup>  
Yu Zhang<sup>3</sup>  
Mei Chen<sup>2</sup>  
Qiang Guo<sup>1-3</sup>  
Wenjing Zhang<sup>1,2,4</sup>

<sup>1</sup>Faculty of Life Science and Biotechnology, Kunming University of Science and Technology, Kunming 650500, People's Republic of China; <sup>2</sup>Medical School, Kunming University of Science and Technology, Kunming 650500, People's Republic of China; <sup>3</sup>Department of Gastroenterology, The First People's Hospital of Yunnan Province, Yunnan Provincial Institute of Digestive Medicine, Kunming 650032, People's Republic of China; <sup>4</sup>Department of Medical Oncology, The First People's Hospital of Yunnan Province, Kunming 650032, People's Republic of China

**Purpose:** Colorectal cancer (CRC) is one of the most commonly occurring cancers and is associated with high morbidity and mortality. Nevertheless, there is currently no safe and effective treatment for this condition. Thymol is a phenolic compound that is recognized as safe for use in food as well as medical and cosmetic fields. Increasing evidence has indicated that thymol exerts prominent antitumor effects in a variety of cancers, including CRC. However, how thymol elicits these effects on CRC and the associated underlying mechanisms remains unclear.

**Methods:** HCT116 and Lovo cells were treated with different concentrations of thymol. Cell Counting Kit-8 (CCK-8) and transwell migration and invasion assays were used to evaluate cell proliferation, migration, and invasion, respectively. Cell apoptosis and cell cycle distribution were measured by flow cytometry. RT-qPCR, Western blot, and immunohistochemistry were used to detect the expression of related genes and their protein products.

**Results:** In this study, we tested the antitumor activity of thymol extracted from a Chinese medicinal herb, *Thymus vulgaris* L. We show that thymol treatment in vitro inhibited cell proliferation and induced apoptosis and cell cycle arrest in CRC. Furthermore, in vivo treatment with 75 and 150 mg/kg thymol led to a significant decrease in tumor volume. Thymol administration induced CRC cell apoptosis through activation of the BAX/Bcl-2 signaling pathway. In addition, thymol suppressed CRC cell epithelial–mesenchymal transition (EMT), invasion, and metastasis via inhibiting the activation of the Wnt/ $\beta$ -catenin pathway, both in vitro and in vivo.

**Conclusion:** Thymol may prevent CRC progression through inhibition of the Wnt/ $\beta$ -catenin signaling pathway, highlighting its potential as a novel therapeutic option for the treatment of CRC.

**Keywords:** Wnt/ $\beta$ -catenin, colorectal cancer, thymol, tumor growth and metastasis

Correspondence: Qiang Guo  
Department of Gastroenterology, The First People's Hospital of Yunnan Province, No. 157 Jinbi Road, Kunming 650032, People's Republic of China  
Tel +86-0871-63634031  
Email gqkj003@sina.com

Wenjing Zhang  
Medical School, Kunming University of Science and Technology, No. 727 South Jingming Road, Kunming 650500, People's Republic of China  
Tel +86-0871-63638481  
Email wenjing\_zhang1@163.com

## Introduction

Colorectal cancer (CRC), also known as bowel cancer, is the third most commonly occurring cancer worldwide.<sup>1,2</sup> In 2012, CRC accounted for more than 1.4 million new cases and 700,000 deaths globally.<sup>3,4</sup> Approximately 30% of CRC patients are diagnosed as stage IV, with a limited median survival of approximately six months if treated only with the best supportive care. Treatments for CRC include surgery, chemotherapy, radiation, or a combination of these. Although significant clinical benefits have been observed with the application of cetuximab and bevacizumab in combination with chemotherapy, CRC morbidity and mortality rates remain high

owing to the high invasive capacity and acquired drug-resistance associated with CRC. Therefore, it is urgent that novel, effective, and less toxic anti-CRC drugs are identified.

The canonical Wnt signaling pathway is highly conserved among metazoans and plays an important role in embryonic development and tumorigenesis.<sup>5</sup> Aberrant activation of Wnt/ $\beta$ -catenin signaling is observed in approximately 90% of patients with CRC.<sup>6,7</sup> Hyperactivation of the Wnt/ $\beta$ -catenin pathway is involved in both the initial and later stages of CRC development, including in tumorigenesis, proliferation, apoptosis, migration, invasion, and epithelial-mesenchymal transition (EMT).<sup>8–10</sup> WNT-protein ligands bind to Frizzled and LRP5/6 membrane receptors to initiate the translocation of  $\beta$ -catenin into the nucleus. Here,  $\beta$ -catenin forms a complex with its co-activators and activates the transcription of downstream target genes such as c-Myc and cyclin D1,<sup>11,12</sup> genes that play key roles in tumorigenesis as well as in cell proliferation, invasion, and migration.<sup>13</sup> EMT is a complex process through which epithelial cells transform and acquire an invasive mesenchymal phenotype, directly contributing to cancer invasion and metastasis.<sup>14</sup> Several studies have revealed that activation of the Wnt/ $\beta$ -catenin signaling pathway can promote cancer metastasis by stimulating EMT dynamic progression,<sup>15,16</sup> whereas disruption of the pathway has been suggested to inhibit cell proliferation, metastasis, and EMT in CRC.<sup>17</sup> This suggests that targeting the Wnt/ $\beta$ -catenin signaling pathway may be an innovative therapeutic approach for the treatment of CRC.

Herbal medicines show great promise as sources of novel anticancer drugs.<sup>18</sup> *Thymus vulgaris* L. is a traditional Chinese herb that possesses multiple biological and pharmacological properties, including antimicrobial, antiseptic, antiviral, and antifungal activities.<sup>19</sup> Thymol is a natural phenolic compound originally isolated and extracted from the essential oils of *T. vulgaris*. Thymol is recognized as safe by the FDA and exhibits antispasmodic, antioxidant, antibacterial, and anti-inflammatory activities.<sup>20–22</sup> Importantly, it also has potential effects against various cancer cells.<sup>23–25</sup> Thymol can inhibit cell invasion and migration in HT29 cells through blocking the phosphorylation of ERK2, p38, and Akt,<sup>26</sup> and can also promote oxidative stress, leading to cell death in the HCT116 CRC cell line.<sup>27</sup> However, the potential mechanisms underlying the antitumor activity of thymol remain unclear.

In this study, we isolated and extracted thymol from *T. vulgaris* and demonstrated that thymol inhibits cell

proliferation, invasion, migration, and EMT, while also inducing cell apoptosis and cell-cycle arrest in CRC cells. We further confirmed the antitumoral role of thymol by inhibiting mouse xenograft tumor formation and lung metastasis in vivo. Mechanistically, thymol suppressed the Wnt/ $\beta$ -catenin signaling pathway as evidenced by changes in the expression of downstream genes. Moreover, we showed that the thymol can partly suppress  $\beta$ -catenin-induced EMT. Overall, our findings describe the antitumoral role of thymol in CRC and the underlying mechanisms, thereby highlighting its potential as a novel therapeutic option for CRC.

## Materials and Methods

### Plant Material

*Thymus vulgaris* L. was collected from Ningxia, China, in June 2018. The identity of the plant was confirmed by Professor Minghua Qiu of the Kunming Institute of Botany, Chinese Academy of Sciences (Kunming, China), where voucher specimens are retained.

### Isolation and Determination of the Active Compound

The air-dried and powdered form of *T. vulgaris* was extracted with methanol for 48 h at room temperature, and then filtered and evaporated. The extract was partitioned between water and ethyl acetate (EtOAc). The EtOAc fraction was applied to silica gel (200–300 mesh) column chromatography, eluted with a gradient system of n-hexane (Hex)–EtOAc (3:1, 2:1, 1:1, 1:2, 1:3), yielding five fractions (1–5). Active components containing the thymol were eluted in fraction 1. Further separation of fraction 1 was performed by silica gel column chromatography, followed by elution with Hex–EtOAc (95:5, 9:1, 8:2), yielding the fractions containing thymol. The fractions were subjected to silica gel column chromatography using Hex–EtOAc (8:2) and semi-preparative HPLC, yielding thymol. The thymol extracted from *T. vulgaris* was dissolved in 100% dimethyl sulfoxide (DMSO) and stored at  $-20^{\circ}\text{C}$ .

### Cell Culture

Human normal colon epithelial (FHC) cells and two CRC cell lines (HCT116 and Lovo) were purchased from Shanghai Cell Biological Institute of the Chinese Academy of Science and maintained in RPMI-1640 medium (Hyclone, Logan, UT, USA) supplemented with 10% fetal bovine serum (Gibco, Australia) and 1% penicillin–streptomycin

(Thermo Fisher Scientific, Waltham, MA, USA) at 37 °C in a humidified incubator with 5% CO<sub>2</sub>.

## Cell Viability and Colony Formation Assay

The effect of thymol on HCT116, Lovo, and FHC cell growth was assessed using CCK-8 assay. Cells were seeded into 96-well plates ( $1 \times 10^4$  cells per well), and incubated until complete adherence. The cells were then treated with a series of thymol concentrations (0, 10, 20, 40, 80, or 120 µg/mL) for the indicated periods (24, 48, or 72 h). CCK-8 (Beyotime Institute of Biotechnology, Shanghai, China) was employed to evaluate cell viability. Optical density at 450 nm was detected using a microplate reader. Cell growth inhibition rates were measured relative to untreated controls, as follows:  $(1 - [\text{OD of drug-treated} - \text{OD of blank}] / [\text{OD of control} - \text{OD of blank}]) \times 100\%$ .

Colony formation assay was used to detect the effect of thymol on colony-forming ability of CRC cells. HCT116 and Lovo cells were plated into 6-well plates (500 cells/well) and treated with thymol at different concentrations (0, 20, or 40 µg/mL) for two weeks until the cells formed visible colonies. The colonies were fixed in 4% paraformaldehyde for 30 min and stained with 0.1% crystal violet. Plates were imaged and colony numbers counted manually.

## Transwell Migration and Invasion Assays

Transwell culture units with 8-µm pore-sized membranes were utilized to detect the effect of thymol on the migratory and invasive ability of CRC cells. For the migration assay, cells were resuspended in serum-free medium and  $1 \times 10^4$  cells were plated into the top chamber. The lower chamber was supplemented with 600 µL of culture medium containing 10% fetal bovine serum. Various concentrations of thymol were added to the upper and lower chambers to a final concentration of 20 or 40 µg/mL. After 24 h of incubation, cells in the top chamber were removed with cotton swabs, and those that had migrated to the lower surface were fixed in 4% paraformaldehyde and stained with 0.1% crystal violet. The stained cells were then observed and counted under a microscope (Zeiss, Germany) at  $\times 100$  magnification. For the invasion assay,  $2 \times 10^4$  CRC cells were added into the upper chamber that had been precoated with Matrigel and treated with various concentrations of thymol for 48 h. The rest of the procedure was as for the migration assay.

## Hoechst 33258 Staining

HCT116 and Lovo cells were seeded and cultured on sterile coverslips in 6-well plates for 24 h. The cells were then treated with different concentrations of thymol (0, 20, or 40 µg/mL) for 48 h. Subsequently, the cells were fixed in 1 mL of 4% paraformaldehyde for 10 min and then 0.5 mL of Hoechst 33258 staining solution (Beyotime) was added to the cells. Finally, apoptotic cells were detected and photographed using a fluorescence microscope (Zeiss) ( $\times 200$ ).

## Flow Cytometric Analysis of Apoptosis

HCT116 and Lovo cells were plated in 6-well plates at a density of  $5 \times 10^5$  cells/well. After 24 h of incubation, cells were exposed to different concentrations of thymol (0, 20, or 40 µg/mL) for 48 h, collected, and stained using an Annexin V-FITC/PI (propidium iodide) apoptosis detection kit (BD Biosciences, Mountain View, CA, USA) for 15 min at 37°C in the dark. The number of apoptotic and necrotic cells was then evaluated using flow cytometry (BD Biosciences).

## Cell Cycle Analysis

HCT116 and Lovo cells were grown in 6-well plates and cultured for 24 h and then treated with thymol at different concentrations (0, 20, or 40 µg/mL) for 48 h. Cells were then harvested, fixed in precooled 70% ethanol at 4°C overnight, and stained with PI/RNase staining buffer (BD Biosciences) for 30 min at room temperature. The cell cycle distribution was analyzed and recorded via flow cytometry (BD Biosciences).

## Western Blot Analysis

Whole-cell and tissue lysates (pooled tissues from each group) were prepared using RIPA lysis buffer. The concentrations of extracted proteins were calculated using BCA kits (Beyotime). Approximately 50 µg of protein was separated by 8–12% SDS-PAGE and transferred to a PVDF membrane. The membrane was then blocked with 10% skimmed milk for 2 h at 37°C. After blocking, the membrane was incubated overnight at 4°C with the following primary antibodies: anti-E-cadherin (1:1,000), anti-vimentin (1:1,000), anti-β-actin (1:1,000), anti-cleaved caspase-3 (1:1,000), anti-cleaved PARP (1:1,000), anti-c-myc (1:1,000), anti-Snail (1:1,000), anti-N-cadherin (1:1,000), anti-cyclin D1 (1:1,000) (all from Cell Signaling Technologies, Boston, USA), anti-BAX (1:800), anti-Bcl-2 (1:800) (both from ProteinTech Group, Chicago,

IL, USA), and anti- $\beta$ -catenin (1:5,000; Abcam, Cambridge, UK). Subsequently, the membranes were incubated with horseradish peroxidase (HRP)-conjugated secondary antibody (Abcam) at 37°C for 2 h. Finally, the protein bands were detected using an ECL detection kit (Merck, Millipore, USA).

## Total RNA Extraction and RT-qPCR

Total RNA was extracted from tumor tissues (pooled tissues from each group) and cells using TRIzol reagent. cDNA was synthesized using the PrimeScript RT reagent kit (Takara, Kyoto, Japan). qPCR reactions were performed on a Light Cycler 480 PCR system using the SYBR Green PCR Master Mix from Takara. The mRNA expression of target genes was normalized to that of GAPDH, and relative target gene expression levels were calculated using the  $2^{-\Delta\Delta CT}$  method. The sequences of the primers used were as follows: Bax: forward, 5'-TTTGCTTCAGGGTTTCA TCC-3' and reverse, 5'-GCCACTCGGAAAAAGACCTC -3'; Bcl-2: forward, 5'-TCGCCCTGTGGATGACTGAG-3' and reverse, 5'-CAGAGTCTTCAGAGACAGCCAGGA -3';  $\beta$ -catenin: forward, 5'-CAACTAAACAGGAAGGGAT GGA-3' and reverse, 5'-CTATACCACCCACTTGGCAG AC-3'; survivin: forward, 5'-TTCTCAAGGACCACCG CATC-3' and reverse, 5'-GCCAAGTCTGGCTCGTTCT C-3'; c-myc: forward, 5'-GGAGGCTATTCTGCCCATTT G-3' and reverse, 5'-CGAGGTCATAGTTCCTGTTGGT G-3'; cyclin D1: forward, 5'-ACAAACAGATCATCCGC AAACAC-3' and reverse, 5'-TGTTGGGGCTCCTCAGG TTC-3'; E-cadherin: forward, 5'-AGGATGACACCCGG GACAAC-3' and reverse, 5'-TGCAGCTGGCTCAAGT CAAAG-3'; snail: forward, 5'-GACCACTATGCCGCGCT CTT-3' and reverse, 5'-TCGCTGTAGTTAGGCTTCCG ATT-3'; vimentin: forward, 5'-AACCTGGCCGAGGACA TCA-3' and reverse, 5'-TCAAGGTCAAGACGTGCCAG A-3'; GAPDH: forward, 5'-GTCAACGGATTTGGTCGTA TTG-3' and reverse, 5'-CTCCTGGAAGATGGTGATGGG -3'. The procedure was performed according to the manufacturer's instructions.

## Plasmids and siRNA Transfection

For  $\beta$ -catenin knockdown analysis, small interfering RNAs (siRNA) targeting  $\beta$ -catenin were designed and synthesized by Shanghai GenePharma Ltd (Shanghai, China; 5'-GGACA CAGCAAUUUGUTT-3') and transfected into CRC cells (HCT116 and Lovo) using Lipofectamine 3000 transfection reagent (Invitrogen, Carlsbad, CA, USA) following the manufacturer's instructions. Scrambled sequences with no

homology to any human gene were used as negative controls. For the overexpression of  $\beta$ -catenin, HCT116 and Lovo cells were transduced with 5  $\mu$ g of a pcDNA3.1- $\beta$ -catenin over-expression plasmid (Shanghai GeneChem Co., Ltd, Shanghai, China); cells transfected with the empty pcDNA3.1 vector served as the control. To confirm that the constructs worked, cells were collected 24 h after transfection and  $\beta$ -catenin protein expression levels were detected by Western blot.

## In vivo Tumor Growth and Metastasis Studies

A total of 28 five-week-old male BALB/c nude (nu/nu) mice were obtained from Hunan SLAC JingDa Laboratory Animal Co., Ltd (Changsha, Hunan, China), and housed under specific pathogen free (SPF) conditions. All the animal experiments were performed according to the guidelines and regulations set by the Animal Care Committee of the First People's Hospital of Yunnan Province. This study was approved by the Animal Care Committee of the First People's Hospital of Yunnan Province.

For the in vivo xenograft model, a total of 16 male nude mice were subcutaneously injected with HCT116 cells ( $1 \times 10^7$  cells in 0.2 mL of PBS) in the back. After 7–10 days, when the tumors had grown to approximately 100 mm<sup>3</sup>, the mice were randomized into four groups (4 mice/group) and received the following treatment by intraperitoneal injection for 30 days: (1) vehicle alone; (2) thymol at 75 mg/kg once every other day; (3) thymol at 150 mg/kg once every other day;<sup>28</sup> or (4) doxorubicin at 2 mg/kg once a week. Thymol was dissolved in vehicle (1% DMSO). Mice in the control group received the same dose of vehicle without thymol. Mice body weights were examined daily during the study period and tumor volumes were measured once every 3 days using a caliper (volume =  $0.5 \times \text{length} \times \text{width}^2$ ). Finally, mice were sacrificed by cervical dislocation following anesthesia using pentobarbital sodium (intraperitoneal injection; 30 mg/kg) and tumor xenografts were removed, weighed, and imaged.

For the lung metastasis model, HCT116 cells ( $1 \times 10^6$ ) were intravenously injected into the tail vein of each mouse. The mice were then randomized into three groups (4 mice/group) and received the following treatment by intraperitoneal injection: (1) vehicle alone; (2) thymol at 75 mg/kg once every other day; or (3) thymol at 150 mg/kg once every other day. Thymol was dissolved in vehicle (1% DMSO). Mice in the control group received the same dose of vehicle without thymol. Six weeks after injection, the mice were

sacrificed by cervical dislocation following anesthesia with pentobarbital sodium (intraperitoneal injection; 30 mg/kg). Lungs were immediately removed and tumors on the lung surface were counted.

## Immunohistochemistry and Hematoxylin and Eosin Staining

The excised tumors and pulmonary tissues were fixed in 4% formaldehyde for 24 h, paraffin-embedded, and sectioned (4- $\mu$ m sections). Tissue sections were deparaffinized and stained with hematoxylin and eosin (H&E) for histological analysis. For immunohistochemistry, after blocking with 5% normal goat serum, sections were incubated with primary antibodies against ki-67 (1:200; Abcam), E-cadherin (1:100),  $\beta$ -catenin (1:100), or vimentin (1:200) (all Cell Signaling Technologies) at 4 °C overnight. Then, the sections were incubated with an HRP-conjugated secondary antibody.

## Statistical Analyses

Data are presented as mean  $\pm$  SD of at least three experiments and analyzed by SPSS 21.0 software (IBM SPSS, Chicago, IL, USA). Statistical analysis among groups was performed by one-way analysis of variance, followed by a Dunnett's multiple comparison post-test. A  $P$ -value  $< 0.05$  was considered significant, and two-sided tests were performed.

## Results

### Thymol Isolation from *T. vulgaris* and Its Structural Characterization

Thymol was isolated from *T. vulgaris* (Figure 1A). Nuclear Magnetic Resonance (NMR) spectroscopy was used to elucidate the chemical structure, and mass spectrometry was performed to identify it as thymol. The spectral data of the isolated substance were as follows:  $^1\text{H}$  NMR (400 Hz,  $\text{CDCl}_3$ ),  $\delta$ : 1.24 (6H, d,  $J=6.9$  Hz, H-9, 10), 2.27 (3H, s, H-7), 3.16 (1H, m,  $J=6.9$  Hz, H-8), 4.61 (1H, s, -OH), 6.58 (1H, s, H-2), 6.73 (1H, d,  $J=7.7$  Hz, H-5), 7.08 (1H, d,  $J=7.6$  Hz, H-4);  $^{13}\text{C}$  NMR (400 Hz,  $\text{CDCl}_3$ ),  $\delta$ : 21.00 (C-7), 22.82 (C-9, 10), 26.89 (C-8), 116.17 (C-2), 121.82 (C-6), 126.39 (C-5), 131.57 (C-4), 136.75 (C-1), 152.69 (C-3). These data are similar to those previously reported.<sup>29</sup>

### Thymol Suppresses Proliferation, Metastasis, and EMT in CRC Cells

To assess the effect of thymol on CRC cells, HCT116 and Lovo cells were treated with thymol at different

concentrations followed by CCK-8 assay. We found that thymol treatment significantly reduced the proliferative capability of HCT116 and Lovo cells in a dose- and time-dependent manner, with  $\text{IC}_{50}$  values of 41.46  $\mu\text{g/mL}$  against Lovo cells and 46.74  $\mu\text{g/mL}$  against HCT116 cells at 48 h (Figure 1B and C). The effect of thymol on FHC cells was also evaluated. As shown in Figure 1D, no cytotoxicity was observed against FHC cells after thymol treatment, even with exposure to the highest concentration tested (120  $\mu\text{g/mL}$ ). These results suggested that thymol inhibits CRC cell proliferation and is not toxic to normal colon epithelial cells. Meanwhile, the colony formation assay showed that the numbers of colonies were decreased in both thymol-treated groups when compared with the respective control groups ( $P < 0.001$ ; Figure 1E). To test the effect of thymol on the migratory and invasive ability of CRC cells, we performed transwell migration and invasion assays. The results of the transwell migration assay showed that thymol inhibited CRC cell migration in a concentration-dependent manner (Figure 1F, left). Consistent with the migration assay, the results of the cell invasion assay showed that thymol treatment could significantly reduce the number of invading CRC cells ( $P < 0.05$ ; Figure 1F, right). These data suggested that thymol exerts an antimetastatic effect in CRC. Since the EMT program is key for cell migration and invasion, we then assessed the effect of thymol on EMT in CRC cells. As shown in Figure 1G, thymol treatment led to a significant increase in the expression of E-cadherin, the most important epithelial EMT marker, whereas the expression of the EMT mesenchymal markers N-cadherin, vimentin, and Snail was reduced.

### Thymol Induces Apoptosis and Cell Cycle Arrest in CRC Cells

Because apoptotic cell death plays an important role in cancer treatment,<sup>30,31</sup> we next investigated whether thymol has an effect on the apoptosis of CRC cells. Hoechst 33258 staining was used to evaluate morphological changes occurring in the nucleus. The results revealed that thymol treatment induced nuclear condensation and fragmentation in a dose-dependent manner (Figure 2A). Flow cytometric analysis was subsequently performed in CRC cells treated or not with thymol. In HCT116 cells, the percentages of apoptotic cells were  $1.5 \pm 0.4\%$  for the control group,  $13 \pm 1.9\%$  for the 20  $\mu\text{g/mL}$  thymol treatment group, and  $21 \pm 1.3\%$  for the 40  $\mu\text{g/mL}$  thymol

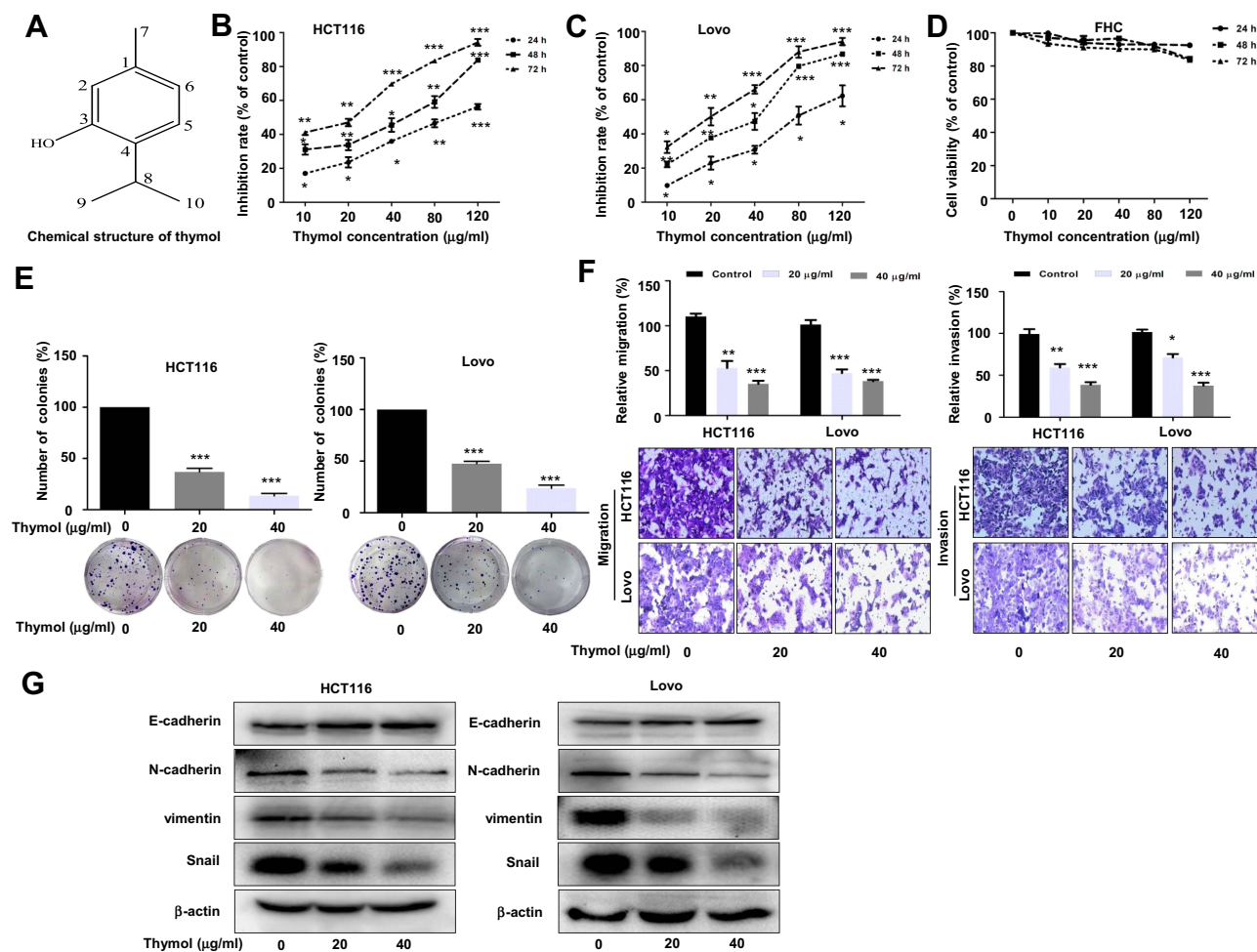


**Figure 1** Thymol suppresses proliferation, migration, invasion, and EMT in colorectal cancer (CRC) cells. **(A)** The chemical structure of thymol. **(B)** Antiproliferative effect of thymol on CRC HCT116 cells. **(C)** Antiproliferative effect of thymol on CRC Lovo cells. **(D)** Effects of thymol on the viability of human normal colon epithelial (FHC) cells. Cells were incubated with different concentrations (0, 10, 20, 40, 80, or 120 μg/mL) of thymol for 24, 48, or 72 h. The CCK-8 assay was used to assess cellular proliferation. DMSO (0.1%) was added as a control. \* $P < 0.05$ , \*\* $P < 0.01$ , \*\*\* $P < 0.001$  vs the control group. **(E)** Representative images from the colony formation assay showing colonies formed by HCT116 and Lovo cells. Cells were treated with thymol at different concentrations (0, 20, or 40 μg/mL). DMSO (0.1%) was added as a control. \*\*\* $P < 0.001$  vs the control group. **(F)** Transwell migration and invasion assays were performed in HCT116 and Lovo cells. Cells were treated with thymol at different concentrations (0, 20, or 40 μg/mL). DMSO (0.1%) was added as a control. Cell migration was assessed at 24 h and invasion at 48 h in both HCT116 and Lovo cells. After migration and invasion, the cells on the lower side of the filter were fixed, stained, and counted. All the images were obtained at a  $\times 100$  magnification. \* $P < 0.05$ , \*\* $P < 0.01$ , \*\*\* $P < 0.001$  vs the control group. **(G)** The expression of EMT-related proteins in thymol-treated CRC cells. E-cadherin, N-cadherin, Snail, vimentin, and  $\beta$ -actin were detected by Western blot in thymol-treated HCT116 and Lovo cells. Beta-actin was used as an internal control. All data are presented as mean  $\pm$  SD of three independent experiments.

treatment group. In Lovo cells, the percentages of apoptotic cells were  $0.8 \pm 0.2\%$  for the control group,  $8 \pm 0.4\%$  for the 20 μg/mL thymol treatment group, and  $20 \pm 1.0\%$  for the 40 μg/mL thymol treatment group (Figure 2B).

To further determine the effect of thymol on CRC cell apoptosis, we performed Western blotting and measured the expression levels of apoptosis-related proteins, including BAX, Bcl-2, cleaved PARP, and cleaved caspase-3. As shown in Figure 2C, thymol treatment led to the upregulation of BAX expression and downregulation of that of Bcl-2, thereby increasing the BAX/Bcl-2 ratio. Similar results were obtained for the RT-qPCR analysis of the mRNA

expression levels of Bcl-2 and BAX ( $P < 0.05$ ; Figure 2D). These results suggested that thymol can trigger mitochondria-dependent apoptosis. The expression levels of cleaved caspase-3 and cleaved PARP were also markedly increased following thymol treatment (Figure 2C).

To determine whether thymol has an effect on cell cycle distribution in CRC, flow cytometry was performed in HCT116 and Lovo cells treated or not with thymol. We found that thymol treatment greatly increased the percentage of cells in the G0/G1 phase and decreased that of cells in the S and G2/M phases (Figure 2E). In HCT116 cells, the percentage of cells in the G0/G1 phase increased from 59% to 79%

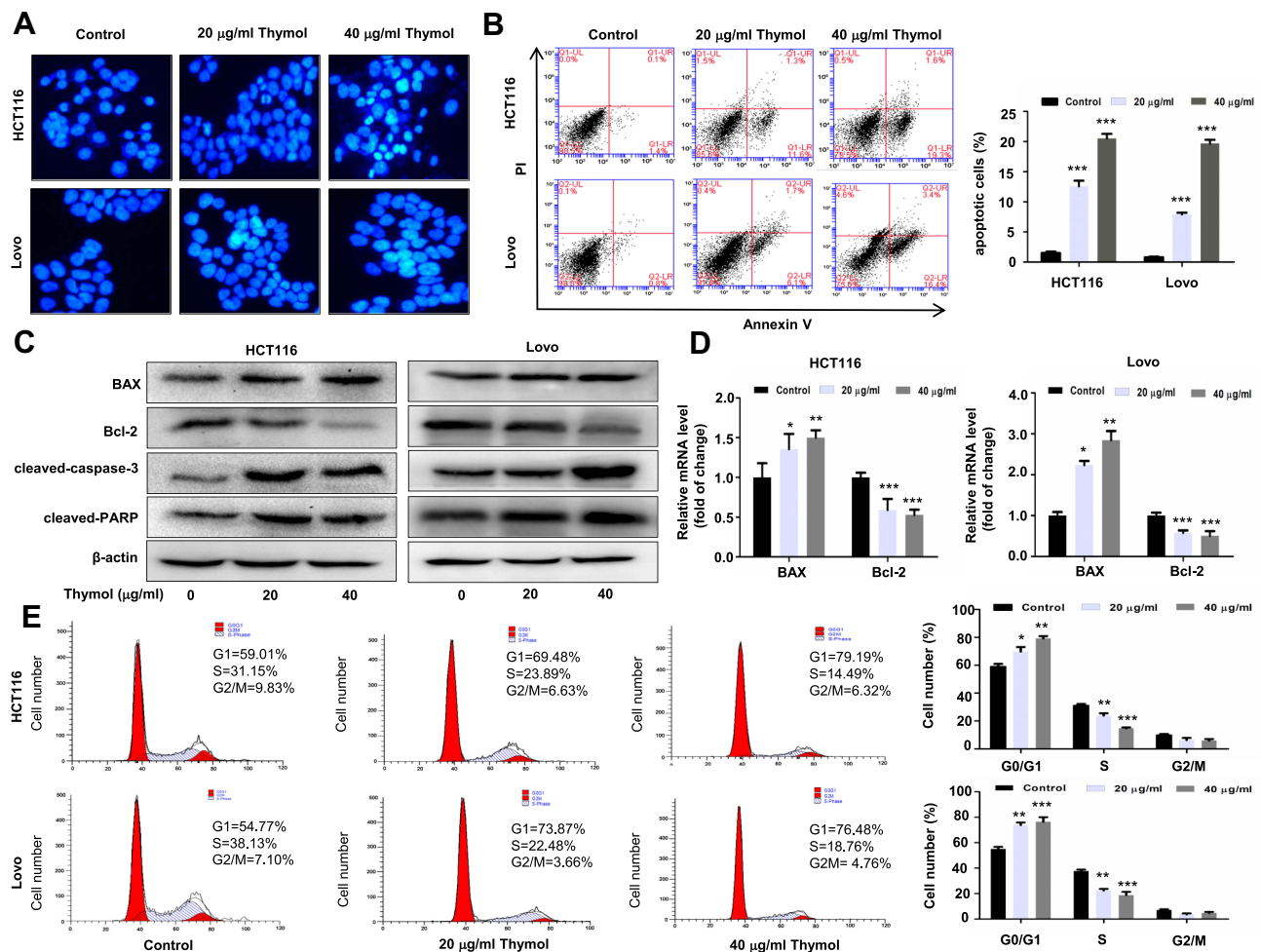


**Figure 2** Thymol induces apoptosis and cell cycle arrest in colorectal cancer (CRC) cells. **(A)** Effects of thymol on the nuclear morphology of CRC cells. Cells were treated with thymol at different concentrations (0, 20, or 40 µg/mL). DMSO (0.1%) was added as a control. After 48 h, the cells were fixed and stained with Hoechst 33258. The morphology of the cancer cells was observed under a fluorescence microscope ( $\times 200$ ). **(B)** Flow cytometric analysis of apoptosis in CRC cells. Thymol treatment promoted cell apoptosis in a dose-dependent manner.  $***P < 0.001$  vs the control group. **(C)** HCT116 and Lovo cells were treated with thymol at different concentrations (0, 20, or 40 µg/mL) for 48 h. DMSO (0.1%) was added as a control. Bcl-2, BAX, cleaved caspase-3, and cleaved PARP protein expression was evaluated by Western blot. **(D)** The mRNA levels of BAX and Bcl-2 were evaluated by RT-qPCR. GAPDH was used as an internal control.  $*P < 0.05$ ,  $**P < 0.01$ ,  $***P < 0.001$  vs the control group. **(E)** Cell cycle analysis by flow cytometry. Cells are treated with thymol at different concentrations (0, 20, or 40 µg/mL). DMSO (0.1%) was added as a control. Thymol treatment shortened the S phase and prolonged the G1 phase in HCT116 and Lovo cells.  $*P < 0.05$ ,  $**P < 0.01$ ,  $***P < 0.001$  vs the control group. All data are presented as mean  $\pm$  SD of three independent experiments.

after thymol treatment, while the percentage of cells in the S phase decreased from 31% to 14% and that of cells in the G2/M phase decreased by 3%. Similar trends were found in Lovo cells. These results suggested that thymol inhibits CRC cell proliferation through changing the cell cycle distribution.

## Thymol Decreases CRC Growth and Metastasis in vivo

To investigate whether thymol is involved in CRC progression, we established a CRC xenograft mouse model by injecting HCT116 cells into BALB/c nude mice. Thymol treatment at both the 75–150 mg/kg concentrations resulted in a significant reduction in CRC growth when

compared with the control group, but there was no significant difference between the group treated with 150 mg/kg thymol and the group treated with doxorubicin used as the positive control (Figure 3A–C). Accordingly, a greater number of necrotic lesions and lower level of Ki-67 expression associated with cell proliferation<sup>32</sup> were observed in mice treated with thymol or doxorubicin when compared with the control group (Figure 3D). Because the Wnt/ $\beta$ -catenin pathway is reported to be hyperactivated in approximately 90% of CRC patients, we then investigated the effect of thymol on Wnt/ $\beta$ -catenin signaling in vivo. For this, we collected the xenograft-derived tumor tissues and measured the expression

levels of  $\beta$ -catenin and its downstream targets, including cyclin D1, c-myc, and survivin, as well as the expression levels of EMT-associated molecules including E-cadherin, N-cadherin, vimentin, and Snail. As shown in Figure 3E and F, the expression levels of  $\beta$ -catenin, cyclin D1, c-myc, and survivin were significantly decreased in mice treated with thymol when compared with those of control mice. Similar results were observed for the expression of N-cadherin, vimentin, and Snail. In contrast, E-cadherin expression was upregulated after thymol treatment. Consistent with our in vitro findings, the expression of BAX was upregulated and that of Bcl-2 downregulated following thymol treatment. Our in vivo data indicated that thymol inhibits CRC growth and metastasis by suppressing Wnt/ $\beta$ -catenin signaling and the EMT program.

To further verify the effect of thymol on CRC metastasis, we established a mouse model of lung metastasis by injecting HCT116 cells into the tail vein of mice. The injected mice were randomized into three groups and treated or not with thymol at the concentration of 75 mg/kg or 150 mg/kg. After six weeks, we found that the average number of tumor nodules on the surface of lungs from the two treatment groups was significantly lower than that in the control group (Figure 4A and B). Similar to the changes observed in the levels of EMT-associated proteins in the xenograft mice, the expression of  $\beta$ -catenin and vimentin was downregulated and that of E-cadherin upregulated in lung metastasis tissues obtained from thymol-treated mice (Figure 4C and D).

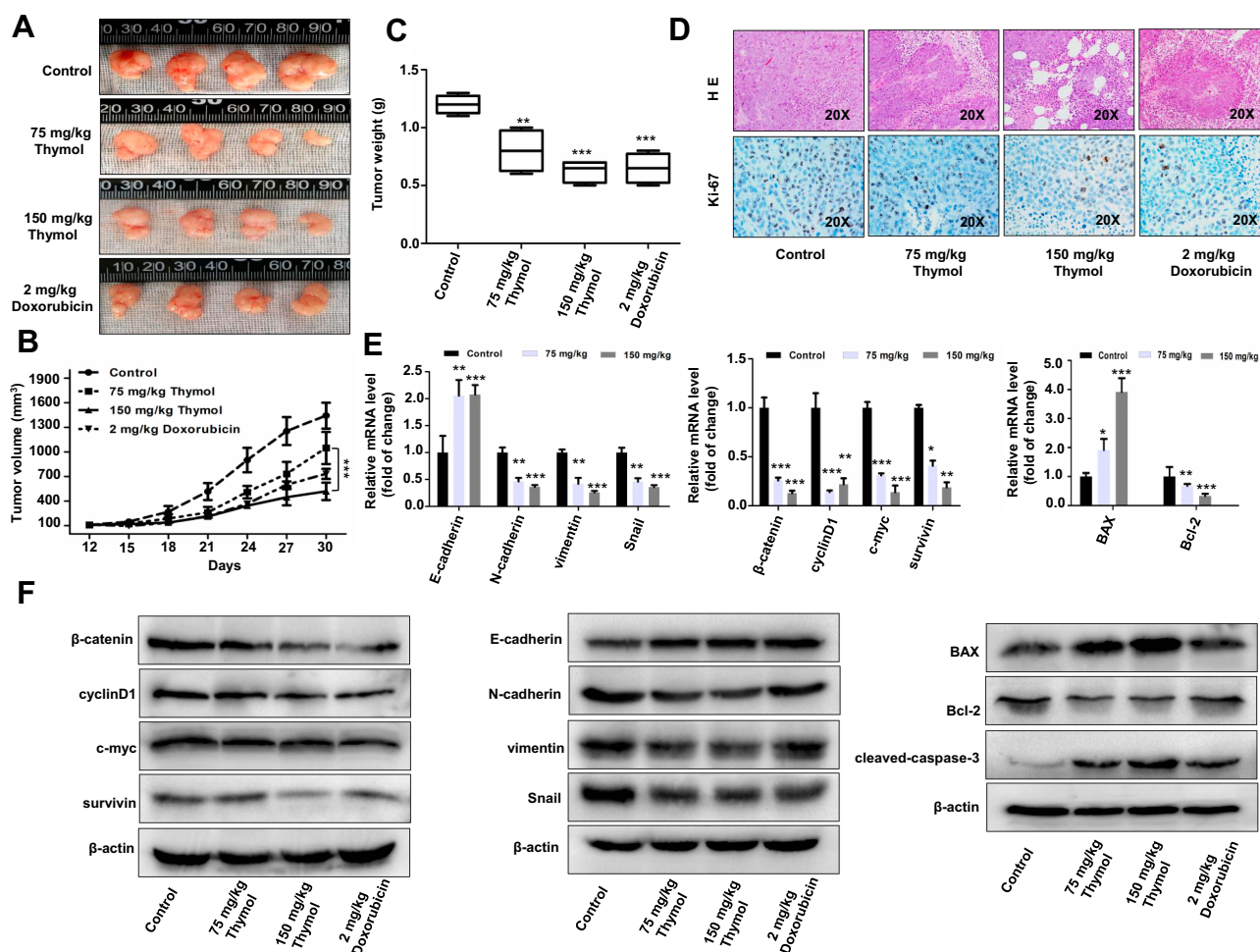


**Figure 3** Thymol inhibits the growth of mouse xenograft colorectal cancer in vivo. Nude mice bearing colorectal cancer cell xenografts were treated with 2 mg/kg doxorubicin once a week and 75 or 150 mg/kg thymol every 2 days. Mice in the control group were treated with saline containing 1% DMSO. (A) Images of nude mice xenograft tumors after 30 days of treatment. (B) Tumor volume of the control, doxorubicin, and thymol treatment groups was measured and calculated once every 3 days. (C) Tumor weight in the control, doxorubicin, and thymol treatment groups. \*\* $P < 0.01$ , \*\*\* $P < 0.001$  vs the control group. (D) Representative histological examinations of the dissected tumors using hematoxylin and eosin (H&E) staining (upper panel) and Ki-67 antibody staining (lower panel) following thymol treatment. RT-qPCR (E) and Western blot (F) analyses were performed to evaluate the expression levels of the indicated mRNAs and proteins, respectively. \* $P < 0.05$ , \*\* $P < 0.01$ , \*\*\* $P < 0.001$  vs the control group. The results are shown as mean  $\pm$  SD from three independent experiments.

## Thymol Inhibits the Wnt/ $\beta$ -Catenin Signaling Pathway

Next, we examined the effect of thymol on the Wnt/ $\beta$ -catenin pathway in vitro. As shown in Figure 5A and B, both the mRNA and protein expression levels of  $\beta$ -catenin, c-myc, cyclin D1, and survivin were significantly down-regulated in thymol-treated HCT116 or Lovo cells compared with the corresponding controls.

## Thymol Inhibits CRC Growth and Metastasis via Suppressing the Wnt/ $\beta$ -Catenin Signaling Pathway

To further evaluate the effect of thymol on the Wnt/ $\beta$ -catenin pathway, we performed loss- and gain-of-function studies. As shown in Figure 6A,  $\beta$ -catenin expression was decreased

after  $\beta$ -catenin siRNA transfection and increased after transfection with a  $\beta$ -catenin-overexpression plasmid in HCT116 and Lovo cells. We found that cotreatment with thymol and  $\beta$ -catenin siRNA synergistically inhibited cell proliferation (Figure 6B, left), invasion, and migration (Figure 6C, left); in contrast, overexpression of  $\beta$ -catenin abolished the inhibitory effect of thymol on cell proliferation (Figure 6B, right), invasion, and migration (Figure 6C, right) in CRC cells. To further clarify the mechanisms underlying the anti-tumoral effect of thymol, we investigated cell apoptosis and invasion-induced gene expression alterations. We found that  $\beta$ -catenin overexpression in HCT116 cells could decrease the expression of BAX and E-cadherin and increase that of Bcl-2, vimentin, and Snail, while thymol treatment could partially reverse these changes (Figure 6D, left). In contrast, thymol and  $\beta$ -catenin siRNA cotreatment synergistically

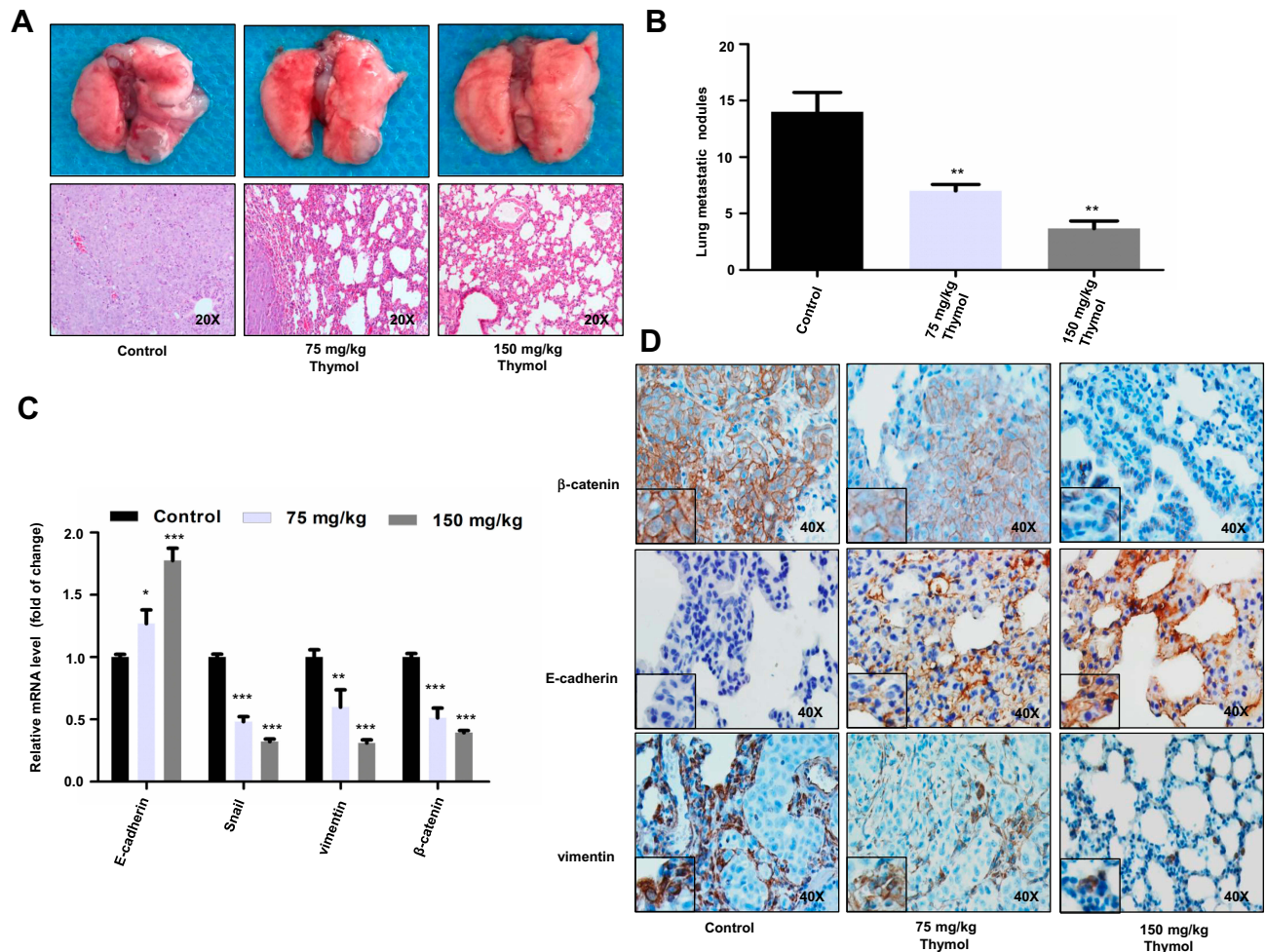


**Figure 4** Thymol reduces colorectal cancer (CRC) lung metastasis. (A) Representative images of lungs with metastatic nodules (upper panel) and images of hematoxylin and eosin (H&E) staining of mouse lung tissues in the control and thymol-treated groups (lower panel). (B) Lung metastatic nodules were examined and quantified in the control and thymol-treated groups. \*\* $P < 0.01$  vs the control group. (C) The mRNA expression levels of E-cadherin, vimentin, Snail, and  $\beta$ -catenin were measured in lung tissues. \* $P < 0.05$ , \*\* $P < 0.01$ , \*\*\* $P < 0.001$  vs the control group. The results are shown as mean  $\pm$  SD from three independent experiments. (D) Representative images of  $\beta$ -catenin, vimentin, and E-cadherin immunohistochemical staining in lung tissues.

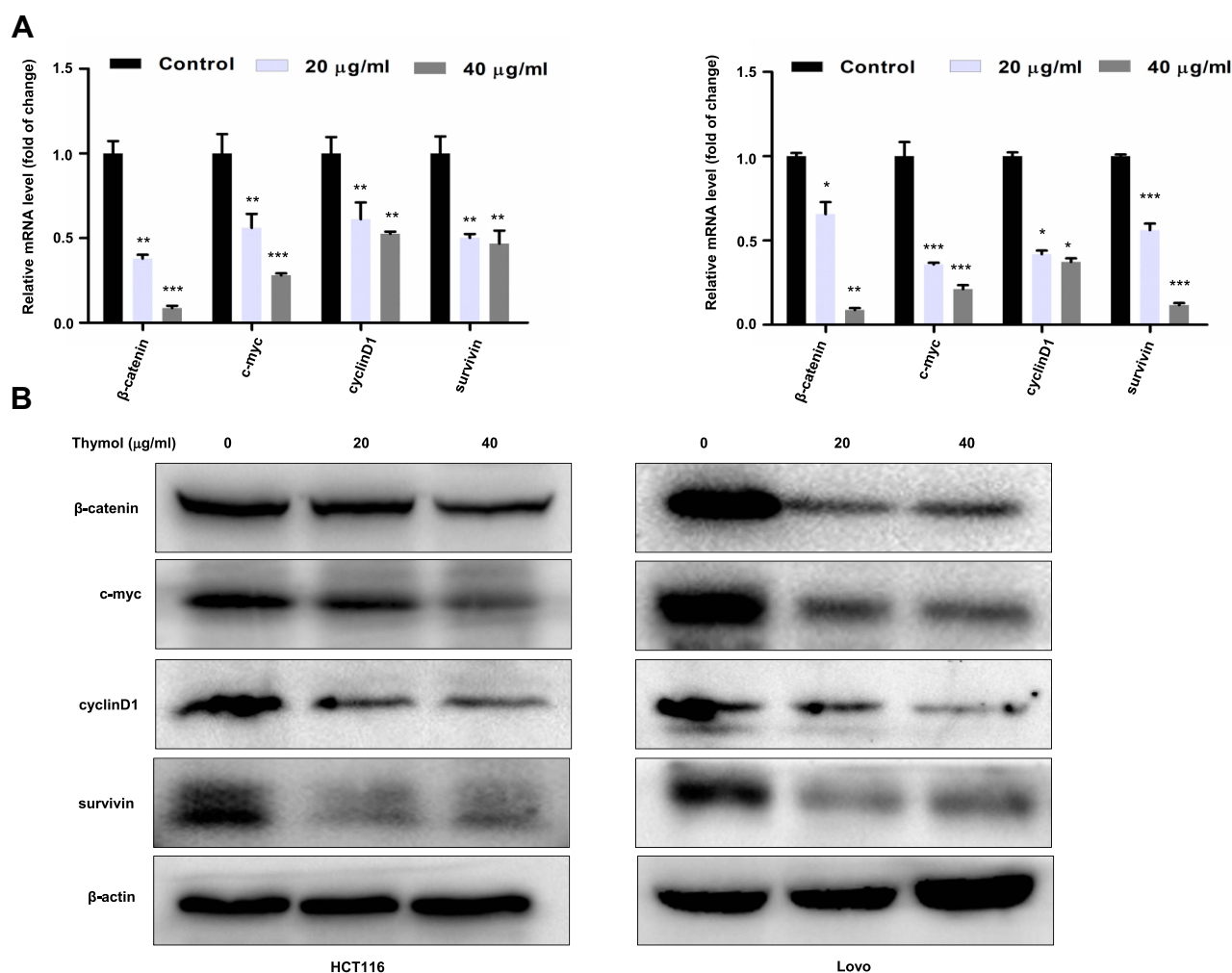


**Figure 5** Thymol suppresses the activation of the Wnt/ $\beta$ -catenin signaling pathway in colorectal cancer (CRC) cells. HCT116 and Lovo cells were treated with different concentrations of thymol (0, 20, or 40  $\mu$ g/ml) for 48 h. DMSO (0.1%) was added as a control. Cell total RNA and proteins were extracted. (A) RT-qPCR was performed to analyze the mRNA expression of  $\beta$ -catenin, c-Myc, cyclin D1, and survivin following thymol treatment. GAPDH was used as an internal control. \* $P$ <0.05, \*\* $P$ <0.01, \*\*\* $P$ <0.001 vs the control group. (B) Western blotting analysis of  $\beta$ -catenin, c-myc, cyclin D1, and survivin protein expression following thymol treatment. Beta-actin was used as an internal control. All data are presented as mean  $\pm$  SD of three independent experiments.

increased the expression of BAX and E-cadherin and decreased that of Bcl-2, vimentin, and Snail (Figure 6D, right). These findings suggested that thymol inhibits CRC cell proliferation, invasion, and migration by suppressing Wnt/ $\beta$ -catenin signaling.

## Discussion

In the present study, we extracted thymol from *T. vulgaris*. Through experiments, we demonstrated that thymol can inhibit cell proliferation, migration, invasion, and EMT in CRC cells; both in vitro and in vivo, indicating that thymol has antitumoral activity against CRC. Moreover, we found that these effects were exerted through inhibition of Wnt/ $\beta$ -catenin pathway activity, as well as regulation of the  $\beta$ -catenin downstream targets cyclin D1, c-myc, and survivin.

Studies have revealed the role of thymol in several types of malignant tumors. In bladder cancer, thymol can significantly induce cell-cycle arrest and apoptosis, thereby inhibiting cell proliferation.<sup>33</sup> Thymol also inhibits human colon cancer cell migration and invasion in vitro, possibly through the activation of the PI3K/AKT and ERK pathways.<sup>26</sup> Additionally, thymol has been shown to promote  $\text{Ca}^{2+}$ -dissociated cell death in PC3 human prostate cancer cells.<sup>34</sup> However, the effective thymol concentrations and the mechanism underlying the effects of thymol in different types of tumors remain uncertain. In the present study, we extracted thymol from *T. vulgaris* and revealed that thymol potently inhibited the proliferative ability of CRC cells with an  $\text{IC}_{50}$  lower than 50  $\mu$ g/mL. Thymol clearly induced cell-cycle arrest and apoptosis,

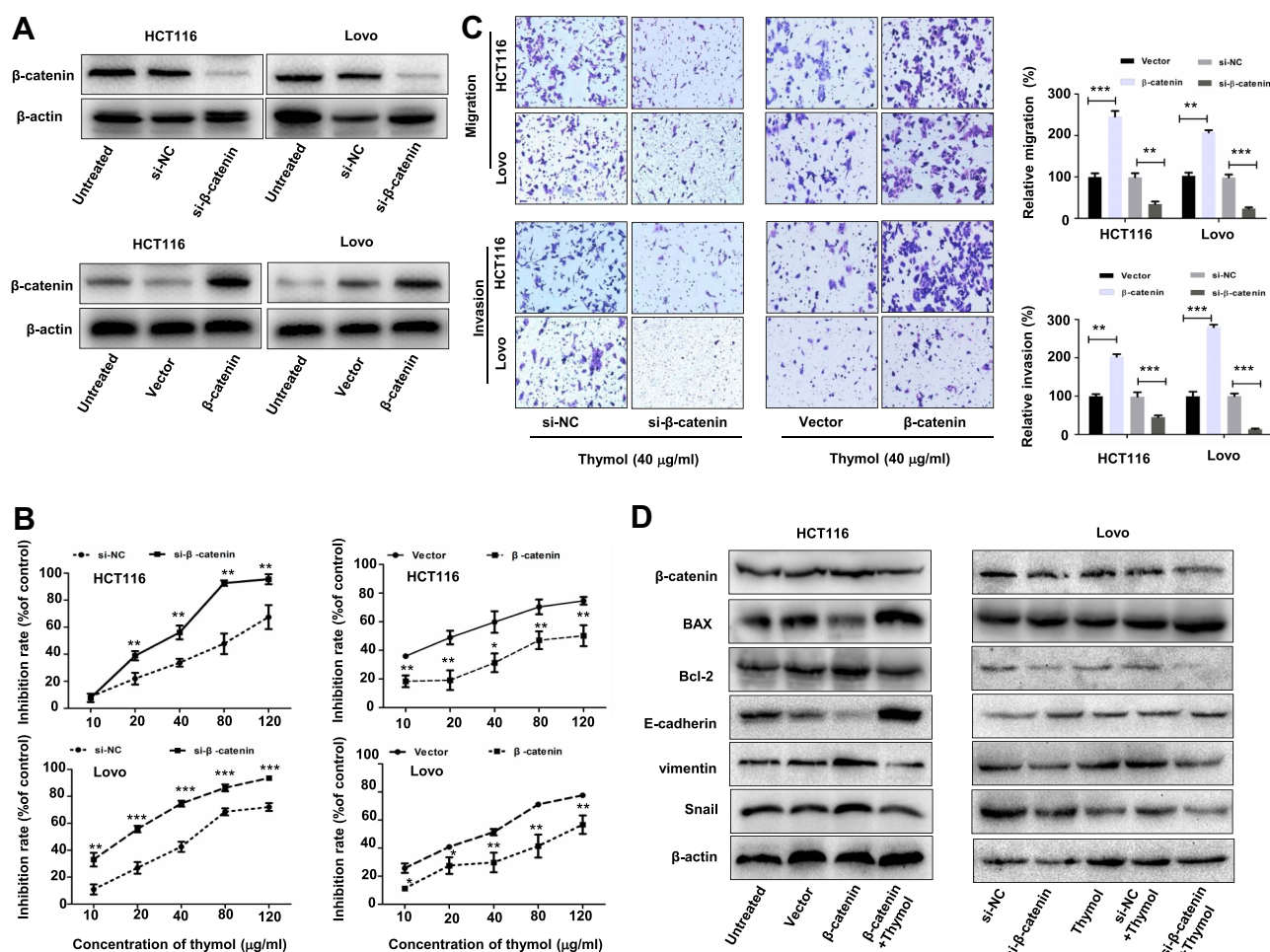


**Figure 6** Thymol inhibits colorectal cancer (CRC) cell proliferation, migration, and invasion by suppressing Wnt/β-catenin signaling. HCT116 and Lovo cells were transfected with β-catenin siRNA (si-β-catenin)/negative control siRNA (si-NC) or the pcDNA3.1-β-catenin plasmid (β-catenin)/pcDNA3.1 (vector). **(A)** Western blot analysis of β-catenin expression in HCT116 and Lovo cells after transfection with β-catenin siRNA, pcDNA3.1-β-catenin, or the corresponding controls for 24 h. **(B)** At 24 h post transfection, the cells were exposed to different concentrations of thymol (0, 10, 20, 40, 80, or 120 μg/mL) and cell proliferation was quantified at 48 h. \* $P < 0.05$ , \*\* $P < 0.01$ , \*\*\* $P < 0.001$  vs the control group. **(C)** At 24 h post transfection, cells were plated into the upper chamber of a transwell plate and treated with thymol (40 μg/mL). After 24 h of incubation, the migratory and invasive abilities were assessed. Cells were stained and imaged under a microscope ( $\times 100$  magnification). \*\* $P < 0.01$ , \*\*\* $P < 0.001$  vs the control group. **(D)** At 24 h post transfection, cells were treated with thymol (40 μg/mL) for 48 h. The expression levels of β-catenin, BAX, Bcl-2, E-cadherin, vimentin, and Snail were measured by Western blotting, and normalized to β-actin expression. All data are presented as mean  $\pm$  SD of three independent experiments.

and significantly suppressed CRC cell migration and invasion in vitro. Importantly, we showed that thymol was noncytotoxic to normal colon epithelial (FHC) cells. Moreover, in vivo, thymol treatment significantly inhibited the growth of subcutaneous CRC xenografts in nude mice, and decreased the number of lung metastatic lesions in mice injected with CRC cells.

Apoptotic cell death has been widely investigated in relation to the treatment of malignant tumors,<sup>35</sup> and thymol has been shown to induce apoptosis and cell cycle arrest in hepatocellular carcinoma cells.<sup>36</sup> We also observed that thymol induced CRC cell apoptosis after 48 h of treatment. Furthermore, we found that thymol treatment clearly decreased the expression level of Bcl-2,

whereas those of BAX, cleaved caspase-3, and cleaved PARP were markedly increased. Expression of Bcl-2 and BAX-family proteins causes the release of cytochrome c, which subsequently activates caspase-3 and PARP, finally resulting in apoptosis.<sup>37</sup> Additionally, similar results were observed in a HCT116 xenograft mouse model, in which tumor development was significantly suppressed compared with that in the control group. mRNA and protein expression of apoptosis-associated molecules extracted from tumors also showed the same tendencies as those of the results obtained in vitro.

Wnt/β-catenin signaling has well-characterized roles in tumorigenesis and metastasis, cancer stem cells, and drug resistance. Beta-catenin is not only the key effector of the

Wnt/ $\beta$ -catenin pathway, but is also an important initiator of the EMT program, a crucial step in cancer metastasis whereby epithelial cells lose their polarity and cell-adhesion properties.<sup>38,39</sup> Accumulated evidence has revealed that activation of the Wnt/ $\beta$ -catenin pathway facilitates EMT, thereby enhancing the invasive and metastatic phenotypes of various tumors by activating transcription factors such as Twist and Snail.<sup>40</sup> Inhibition of  $\beta$ -catenin expression leads to the downregulation of Wnt/ $\beta$ -catenin signaling activity. In the current study, we observed that thymol treatment could downregulate the expression levels of vimentin, Snail, and N-cadherin, and upregulate those of E-cadherin. Furthermore, we showed that thymol significantly downregulated  $\beta$ -catenin levels in CRC cells, resulting in significant decreases in the expression of downstream targets such as cyclin D1, c-myc, and survivin. Following thymol treatment, the levels of Wnt/ $\beta$ -catenin pathway components and EMT markers, including vimentin, Snail, and N-cadherin, were also significantly downregulated, whereas those of E-cadherin were markedly increased, in both CRC xenograft tumor tissues and lung tissues with tumor metastatic nodules. Importantly,  $\beta$ -catenin knock-down significantly enhanced the thymol-mediated inhibition of the proliferative and metastatic potential of CRC cells. Conversely, ectopic overexpression of  $\beta$ -catenin not only significantly neutralized the antiproliferative effect of thymol, but also attenuated the thymol-induced motility restriction in CRC cells. These results suggested that disruption of the Wnt/ $\beta$ -catenin pathway may be the primary mechanism underlying the thymol-mediated antiproliferative and antimetastatic effects in CRC.

## Conclusions

Collectively, our results showed that thymol, a natural product derived from Chinese herbal medicine, inhibited CRC cell proliferation and metastasis and induced cell apoptosis and cell-cycle arrest. Our data further indicated that thymol likely exerts these effects by suppressing the Wnt/ $\beta$ -catenin signaling pathway. Our study showed that thymol is safe and has good anticancer effects, and highlights that thymol has potential for use in the treatment of CRC.

## Funding

This study was supported by grants from the National Natural Science Foundation of China (81860509) and Joint Foundation of Kunming Medical University and Yunnan Provincial Science and Technology Department

(2017FE467-159), and grants from the Internal Division of Yunnan Provincial Health Commission (2016NS226, 2017NS249) and Yunnan provincial foundation for medical academic leader (D-2017002, 2018HB049).

## Disclosure

The authors report no conflicts of interest in this work.

## References

1. Siegel RL, Miller KD, Jemal A. Cancer statistics, 2019. *CA Cancer J Clin*. 2019;69(1):7–34. doi:10.3322/caac.21551
2. Bray FI, Ferlay J, Soerjomataram I, Siegel RL, Torre LA, Jemal A. Global cancer statistics 2018: GLOBOCAN estimates of incidence and mortality worldwide for 36 cancers in 185 countries. *CA Cancer J Clin*. 2018;68(6):394–424. doi:10.3322/caac.21492
3. Navarro M, Nicolas A, Ferrandez A, Lanás A. Colorectal cancer population screening programs worldwide in 2016: an update. *World J Gastroenterol*. 2017;23(20):3632–3642. doi:10.3748/wjg.v23.i20.3632
4. McGuire S World Cancer Report 2014. Geneva, Switzerland: World Health Organization, international agency for research on cancer. 2015. *Adv Nutr*. 2016;7:418–419.
5. Kafka A, Basickinda S, Pecinaslaus N. The cellular story of dishevelleds. *Croat Med J*. 2014;55(5):459–467. doi:10.3325/cmj.2014.55.459
6. Zhou FQ, Qi YM, Xu H, Wang QY, Gao XS, Guo HG. Expression of EpCAM and Wnt/ $\beta$ -catenin in human colon cancer. *Genet Mol Res*. 2015;14(2):4485–4494. doi:10.4238/2015.May.4.6
7. Nie X, Xia F, Liu Y, et al. Downregulation of Wnt3 suppresses colorectal cancer development through inhibiting cell proliferation and migration. *Front Pharmacol*. 2019;10:1110–1123. doi:10.3389/fphar.2019.01110
8. Nusse R, Clevers H. Wnt/ $\beta$ -Catenin signaling, disease, and emerging therapeutic modalities. *Cell*. 2017;169(6):985–999. doi:10.1016/j.cell.2017.05.016
9. Jiang Z, Zhang Y, Chen X, Wu P, Chen D. Inactivation of the Wnt/ $\beta$ -catenin signaling pathway underlies inhibitory role of microRNA-129-5p in epithelial–mesenchymal transition and angiogenesis of prostate cancer by targeting ZIC2. *Cancer Cell Int*. 2019;19:271. doi:10.1186/s12935-019-0977-9
10. Basu S, Haase G, Ben-Ze'ev A. Wnt signaling in cancer stem cells and colon cancer metastasis. *F1000Res*. 2016;5:F1000 Faculty Rev–699. doi:10.12688/f1000research.7579.1
11. Minde D, Radli M, Forneris F, Maurer MM, Rüdiger SG. Large extent of disorder in adenomatous polyposis coli offers a strategy to guard wnt signalling against point mutations. *PLoS One*. 2013;8(10):e77257–e77266. doi:10.1371/journal.pone.0077257
12. Valenta T, Hausmann G, Basler K. The many faces and functions of  $\beta$ -catenin. *EMBO J*. 2012;31(12):2714–2736. doi:10.1038/emboj.2012.150
13. Clevers H, Nusse R. Wnt/ $\beta$ -Catenin signaling and disease. *Cell*. 2012;149(6):1192–1205. doi:10.1016/j.cell.2012.05.012
14. Tsuji T, Ibaragi S, Hu G. Epithelial-mesenchymal transition and cell cooperativity in metastasis. *Cancer Res*. 2009;69(18):7135–7139. doi:10.1158/0008-5472.CAN-09-1618
15. Wang B, Sun L, Li J, Jiang R. miR-577 suppresses cell proliferation and epithelial-mesenchymal transition by regulating the WNT2B mediated Wnt/ $\beta$ -catenin pathway in non-small cell lung cancer. *Mol Med Rep*. 2018;18(3):2753–2761. doi:10.3892/mmr.2018.9279
16. Siar CH, Ishak I, Ng KH. Podoplanin, E-cadherin,  $\beta$ -catenin, and CD44v6 in recurrent ameloblastoma: their distribution patterns and relevance. *J Oral Pathol Med*. 2015;44(1):51–58. doi:10.1111/jop.12203

17. Han P, Li J, Zhang B, et al. The lncRNA CRNDE promotes colorectal cancer cell proliferation and chemoresistance via miR-181a-5p-mediated regulation of Wnt/ $\beta$ -catenin signaling. *Mol Cancer*. 2017;16(1):9. doi:10.1186/s12943-017-0583-1
18. Newman DJ, Cragg GM. Natural products as sources of new drugs over the 30 years from 1981 to 2010. *J Nat Prod*. 2012;75(3):311–335. doi:10.1021/np200906s
19. Sokovic M, Glamoclija J, Ciric A, et al. Antifungal activity of the essential oil of *Thymus vulgaris* L. and thymol on experimentally induced dermatomycoses. *Drug Dev Ind Pharm*. 2008;34(12):1388–1393. doi:10.1080/03639040802130053
20. Meeran MF, Javed H, Taeq HA, Azimullah S, Ojha SK. Pharmacological properties and molecular mechanisms of thymol: prospects for its therapeutic potential and pharmaceutical development. *Front Pharmacol*. 2017;8:380. doi:10.3389/fphar.2017.00380
21. Marchese A, Orhan IE, Daglia M, et al. Antibacterial and antifungal activities of thymol: a brief review of the literature. *Food Chem*. 2016;210:402–414. doi:10.1016/j.foodchem.2016.04.111
22. Xie K, Tashkin DP, Luo MZ, Zhang JY. Pharmacokinetic study of thymol after intravenous injection and high-dose inhalation in mouse model. *Pharmacol Res Perspect*. 2019;7(5):e00515–e00523. doi:10.1002/prp2.515
23. Deb DD, Parimala G, Devi SS, Chakraborty T. Effect of thymol on peripheral blood mononuclear cell PBMC and acute promyelocytic cancer cell line HL-60. *Chem Biol Interact*. 2011;193(1):97–106. doi:10.1016/j.cbi.2011.05.009
24. Gunesbayir A, Kiziltan HS, Kocyigit A, Güler EM, Karataş E, Toprak A. Effects of natural phenolic compound carvacrol on the human gastric adenocarcinoma (AGS) cells in vitro. *Anticancer Drugs*. 2017;28(5):522–530. doi:10.1097/CAD.0000000000000491
25. La Chapa JJ, Singha PK, Lee DR, Gonzales CB. Thymol inhibits oral squamous cell carcinoma growth via mitochondria-mediated apoptosis. *J Oral Pathol Med*. 2018;47(7):674–682. doi:10.1111/jop.12735
26. Lv R, Chen Z. Thymol inhibits cell migration and invasion by down-regulating the activation of PI3K/AKT and ERK pathways in human colon cancer cells. *Trop J Pharm Res*. 2018;16(12):2895–2901. doi:10.4314/tjpr.v16i12.13
27. Chauhan AK, Bahuguna A, Paul S, Kang SC. Thymol Elicits HCT-116 colorectal carcinoma cell death through induction of oxidative stress. *Anticancer Agents Med Chem*. 2017;17(14):1942–1950.
28. Hosseinimehr SJ, Asadian R, Naghshvar F, et al. Protective effects of thymol against nephrotoxicity induced by cisplatin with using <sup>99m</sup>Tc-DMSA in mice. *Ren Fail*. 2015;37(2):280–284. doi:10.3109/0886022X.2014.991998
29. Okazaki K, Kawazoe K, Takaishi Y. Human platelet aggregation inhibitors from thyme (*Thymus vulgaris* L.). *Phytother Res*. 2002;16(4):398–399. doi:10.1002/ptr.979
30. Lin Y, Shen Y, Wu C, et al. Danshen improves survival of patients with breast cancer and dihydroisotanshinone i induces ferroptosis and apoptosis of breast cancer cells. *Front Pharmacol*. 2019;10:1226–1239. doi:10.3389/fphar.2019.01226
31. Lou C, Chen Y, Zhang J, Yang B, Zhao H. Eupalinolide J suppresses the growth of triple-negative breast cancer cells via targeting STAT3 signaling pathway. *Front Pharmacol*. 2019;10:1071–1086. doi:10.3389/fphar.2019.01071
32. Sulik M, Maruszak K, Puchalska J, Misiukiewicz-Poć M. Expression of Ki-67 as a proliferation marker in prostate cancer. *Polish Ann Med*. 2011;18(1):12–19. doi:10.1016/S1230-8013(11)70019-4
33. Li Y, Wen J, Du C, et al. Thymol inhibits bladder cancer cell proliferation via inducing cell cycle arrest and apoptosis. *Biochem Biophys Res Commun*. 2017;491(2):530–536. doi:10.1016/j.bbrc.2017.04.009
34. Yeh J, Chou C, Chen IS, et al. Effect of thymol on Ca<sup>2+</sup> homeostasis and viability in PC3 human prostate cancer cells. *Chin J Physiol*. 2017;60(1):32–40. doi:10.4077/CJP.2017.BAF447
35. Huang C, Yang G, Jiang T, Cao J, Huang KJ, Qiu ZJ. Down-regulation of STAT3 expression by vector-based small interfering RNA inhibits pancreatic cancer growth. *World J Gastroenterol*. 2011;17(25):2992–3001. doi:10.3748/wjg.v17.i25.2992
36. Mansour M, Mohamed MF, Elhalwagi A, El-Itriby HA, Shawki HH, Abdelhamid IA. *Moringa peregrina* leaves extracts induce apoptosis and cell cycle arrest of hepatocellular carcinoma. *Biomed Res Int*. 2019;2019:2698570–2698583. doi:10.1155/2019/2698570
37. Edlich F, Banerjee S, Suzuki M, et al. Bcl-xL retrotranslocates Bax from the mitochondria into the cytosol. *Cell*. 2011;145(1):104–116. doi:10.1016/j.cell.2011.02.034
38. Craene BD, Berx G. Regulatory networks defining EMT during cancer initiation and progression. *Nat Rev Cancer*. 2013;13(2):97–110. doi:10.1038/nrc3447
39. Rashed HE, Hussein S, Mosaad H, et al. Prognostic significance of the genetic and the immunohistochemical expression of epithelial-mesenchymal-related markers in colon cancer. *Cancer Biomark*. 2017;20(1):107–122. doi:10.3233/CBM-170034
40. Xie SL, Fan S, Zhang SY, et al. SOX8 regulates cancer stem-like properties and cisplatin-induced EMT in tongue squamous cell carcinoma by acting on the Wnt/ $\beta$ -catenin pathway. *Int J Cancer*. 2018;142(6):1252–1265. doi:10.1002/ijc.31134

## Drug Design, Development and Therapy

### Publish your work in this journal

Drug Design, Development and Therapy is an international, peer-reviewed open-access journal that spans the spectrum of drug design and development through to clinical applications. Clinical outcomes, patient safety, and programs for the development and effective, safe, and sustained use of medicines are a feature of the journal, which has also

been accepted for indexing on PubMed Central. The manuscript management system is completely online and includes a very quick and fair peer-review system, which is all easy to use. Visit <http://www.dovepress.com/testimonials.php> to read real quotes from published authors.

Submit your manuscript here: <https://www.dovepress.com/drug-design-development-and-therapy-journal>

Dovepress